

X-ray observations of the young open cluster Blanco 1

G. Micela¹, S. Sciortino¹, F. Favata², R. Pallavicini¹, and J. Pye³

¹ Osservatorio Astronomico di Palermo, Palazzo dei Normanni, I-90134 Palermo, Italy (gmicela; ssciortino; pallavic@oapa.astropa.unipa.it)

² Astrophysics Division – Space Science Department of ESA, ESTEC, Postbus 299, 2200 AG, Noordwijk, The Netherlands (ffavata@astro.estec.esa.nl)

³ Department of Physics and Astronomy, Leicester University, UK (pye@star.le.ac.uk)

Received 18 August 1998 / Accepted 1 December 1998

Abstract. We present results from two deep ROSAT HRI exposures on the Blanco 1 open cluster. Blanco 1 is one of the few open clusters at large distance from the Galactic Plane. This circumstance has suggested that it may have formed through a mechanism different from that responsible for the other nearby clusters. The age of Blanco 1 is rather uncertain since, depending on the adopted age indicator, it ranges between 30 and 90 Myr. Many cluster members show chromospheric emission typical of young stars. The X-ray observations presented here reveal a high number of X-ray sources, consistent with the young age of the cluster. The typical X-ray luminosity of the cluster members is consistent with that of the Pleiades and significantly lower than the α Per members. These results suggest that the age of Blanco 1 is more similar to the age of the Pleiades than to that of α Per.

The time sampling of the X-ray observations allows us to study the variability of the sources on time scales from hours to 6 months – 1 year.

Key words: X-rays: stars – stars: coronae – Galaxy: open clusters and associations: individual: Blanco 1

1. Introduction

X-ray observations of open clusters have allowed us to explore the activity-age-rotation connection in the coronal domain. A large number of clusters with ages ranging from those of star-forming regions to that of the Hyades have been studied, mainly through ROSAT observations (see for example Randich 1997 and references therein), producing a consistent picture of X-ray activity decreasing with age as the rotational velocity of stars decreases with age. The faster rotators, more frequent in the youngest clusters, appear to be in a “saturated” state with a typical value of $\log L_X/L_{\text{bol}} \approx -3$, independent of rotation. On the contrary, the activity level of the slowest rotators is related to the stellar rotation with a power law similar to that observed in the nearby (and older) field stars (Pallavicini et al. 1981). Stars with an age similar to that of the Pleiades seem to be in an intermediate state in the sense that the rotation distribution of the dG stars is dominated by the slow rotators (for which a relation

$L_X - \text{rotation}$ holds) while the dK stars are dominated by fast rotators in the “saturated” regime. Exceptions to this apparently well established behavior have been observed. For example the G stars in Praesepe are significantly under-luminous with respect to the G stars in the Hyades, even though they have the same stellar properties (including rotation, Mermilliod 1997) and age. For this reason the study of other clusters can add new elements in order to explain this puzzling behavior.

On the other hand X-ray surveys demonstrated to be a powerful means to find new cluster members in young clusters and stellar associations, on the low-mass end of the mass function. The high X-ray activity level of young stars makes X-ray surveys more successful than traditional techniques in picking up cluster members mainly because they are less contaminated by the field population. In this context X-ray observations can help very effectively in deriving the Initial Mass Function (IMF) of young clusters.

The HR diagram of Blanco 1 (ζ Sculptoris) indicates that its age is similar to that of the Pleiades. In the most complete study of this cluster, de Epstein & Epstein (1985) have obtained photographic photometry of about 1500 stars down to $m_V \approx 16.5$ (corresponding to the late dK cluster members). Spectral types are available down to early G members and are missing for redder stars. From the analysis of the derived color-magnitude (CM) diagram, de Epstein & Epstein (1985) conclude that about 150 of the stars in their study belong to the cluster main sequence and deduce a distance modulus of 6.9 mags (i.e. a distance of 240 pc) and a color excess $E(B - V) = 0.013$. Up to now membership has been based only on photometric criteria, lacking astrometric studies of the cluster, and preventing complete studies of members, in particular of low-mass stars.

In the last few years some studies of Blanco 1 have shown that while photometric indicators such as m_1 or $U - B$ seem to imply a metal-poor cluster (de Epstein & Epstein, 1985; Westerlund et al. 1988), the detailed analysis of high resolution spectroscopic observations (Edvardsson et al. 1995) results in a metal abundance $[\text{Fe}/\text{H}] = +0.23$, about 70% higher than the solar value. Furthermore they report a peculiarly high $[\text{Ni}/\text{Fe}]$ abundance.

Analogous contradictory results between photometric and spectroscopic abundances seem to be common in very active

Table 1. Summary of the HRI observations

Field	RA(J2000) (h m s)	DEC(J2000) ° ' "	LIVE-TIME (sec)	UT START DATE	UT END DATE
1	00 02 48.0	−30 00 00.0	32028	21-DEC-95/09:34:09	26-DEC-95/12:52:02
			17820	22-JUN-96/03:43:43	23-JUN-96/09:02:07
			38392	28-NOV-96/23:34:27	29-NOV-96/16:47:42
2	00 05 36.0	−30 06 00.0	71120	30-NOV-96/12:18:10	7-DEC-96/20:32:27

stars in which the Strömgren m_1 index produces an apparent metal deficiency (Pettersen 1982, Jetsu et al. 1990, Gimenez et al. 1991). A similar apparent metal deficiency has been reported by Giampapa (1979) comparing the m_1 index measured in active solar regions with the same index measured in more quiet solar regions. A program of Strömgren photometric observations of an X-ray selected stellar sample from the *Einstei*n Extended Medium Sensitivity Survey (EMSS, Gioia et al. 1990) has shown that the m_1 index of otherwise “normal” main-sequence G and K dwarfs is indeed affected by activity, with m_1 deficiency (with respect to the predicted main-sequence value) increasing with f_X/f_V (see Fig. 1 from Morale et al. 1996). This behavior cannot be explained by the occurrence of a large fraction of active binaries but is due to intense activity associated with the young age of most of the studied stars. Also in this case spectroscopic observations have shown (Favata et al. 1997) that the metallicity of these stars is similar to or greater than the solar one.

Panagi et al. (1994) have presented spectroscopic observations of a sizeable fraction of cluster members, covering the whole bandpass from the Ca II H and K region to the Ca II IR triplet. These authors find a high mean Ca II surface flux consistent with that of other young clusters and deduce the presence of a high degree of surface inhomogeneity, implying intense magnetic activity on young stars. Lithium observations indicate that Blanco 1 has an age similar to that of the young cluster α Persei (Panagi et al. 1994, Panagi & O’Dell 1997), but since lithium is a crude estimator of age, it is impossible to better determine the cluster age. On the contrary the relatively small number of H α emitters seems to indicate a cluster age slightly older than the Pleiades i.e. 90 ± 25 Myr (Panagi & O’Dell 1997).

The age estimate based on CM diagram indicates that the cluster is very young with an age in the 30 Myr (Westerlund 1988) to 50 Myr (de Epstein & Epstein 1985) range. Panagi & O’Dell note that this young age is based only on the membership of the B8 star HD 225187, that is the bluest star of the cluster. Perry et al. (1978) note that the star has a proper motion not completely consistent with that of the cluster and suspect that the star is a spectroscopic binary since it has variable radial velocity. The membership of this star is crucial in assessing whether the cluster age is less than 50 Myr (if the B8 star belongs to the cluster) or greater than that of the Pleiades (if the B8 star does not belong to the cluster).

Blanco 1 is also one of the few open clusters at high galactic latitude; the formation mechanism of such systems is unclear. Based on the large distance from the Galactic Plane (240 pc) and

on its age, Edvardsson et al. (1995) suggest that the cluster has been formed near the disk ≈ 45 Myr ago by a stellar formation process triggered by the interaction of a high velocity cloud with the interstellar medium in the disk. This origin could explain the large distance of the cluster from the Plane. Edvardsson et al. (1995) also suggest a possible common origin of Blanco 1 and the Gould Belt, and that the peculiar chemical composition they found in the cluster could be due to the composition of the original gas, far away from the solar neighborhood. Another cluster far away from the Galactic Plane is IC4665 which is ≈ 100 pc distant from the Galactic Plane, and has been studied in X-rays by Giampapa et al. (1998).

In the context of its unique characteristics, an X-ray survey of Blanco 1 is interesting in order to investigate further the X-ray evolution of solar-type stars since this cluster seems to have an origin different (Edvardsson et al. 1995) than other more studied clusters of similar age.

Our paper is organized as follows: Sect. 2 presents the observations and data analysis, Sect. 3 presents the X-ray properties of cluster members, Sect. 4 discusses the X-ray variability of the cluster members. The properties of unidentified cluster members are presented in Sect. 5 and our results are summarized in Sect. 6.

2. X-ray observations and data analysis

We have obtained 2 deep adjacent HRI observations pointed toward the central part of the Blanco I cluster. One of the two images (hereafter Field 1) has been observed in three distinct segments 6 months apart. Table 1 gives a summary of the X-ray observations and Figs. 1 and 2 show the images with overimposed the sources detected as described below. The size of the HRI field of view ($\approx 40' \times 40'$) allows us to cover a sizeable fraction of the cluster.

The explored area contains 83 member stars out of the total 210 stars considered as members by Panagi & O’Dell (1997).

All the HRI data have been analyzed adopting a wavelet transform detection algorithm (Damiani et al. 1997a,b) specifically tuned for the characteristics of the HRI detector (Damiani et al. in prep.) that allows an efficient detection of weak sources in crowded fields even in the presence of spatially variable background, and which provides source intensity, probability of existence and extent. In particular the images have been flat-fielded using both the exposure map (which models the vigneted cosmic X-ray background and the intrinsic detector nonuniformities) and particle map (which models particle-induced back-

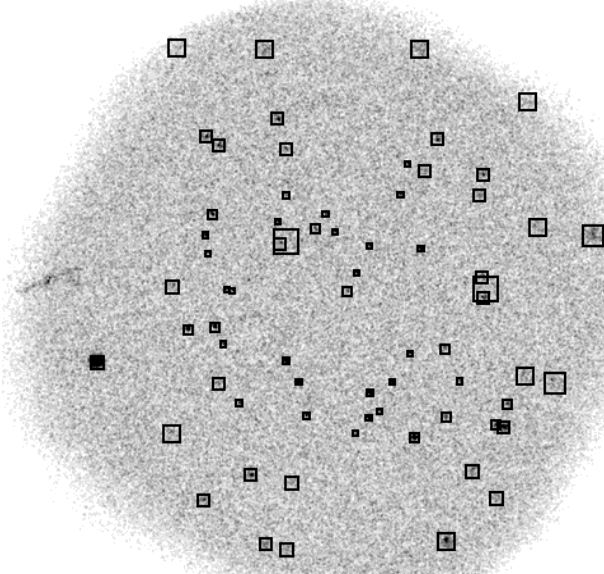


Fig. 1. X-ray map of Field 1. The squares represent the detections obtained as described in the text. The size of the squares is proportional to the scale at which the source has been detected with the highest significance. Note the presence of some extended sources. The strip on the left of the image is due to the detector hot spot.

ground that increases at large off-axis angles and contributes a substantial fraction of the total observed background) generated as described in Snowden (1998) and Snowden et al. (1994), and adopting the Point Spread Function (PSF) of David et al. (1993). The detection algorithm has been applied on nine different spatial scales to match the variation of the PSF across the field of view and to look for possible presence of moderately extended sources. In the present work the detection algorithm acceptance threshold, determined through extensive simulations, has been chosen to correspond roughly to a gaussian equivalent of 4.5σ , in order to have no-more than one predicted spurious source for each HRI image.

Sources have been searched in Field 2 and in each of the three segments making the entire Field 1 observation. Before proceeding with the analysis of the summed Field 1 observation, we have searched for possible inconsistencies of the aspect determination among the three segments, since this is a well known problem affecting the ROSAT HRI observations (Briel et al. 1996). Using as reference coordinate system that of the optical positions of the cluster members, we have identified the likely counterparts of X-ray sources in each of the three segments and have found a misplacement up to $12''$ among the three segments. The adopted identification radius has been chosen equal to $20''$ to account for uncertainties in X-ray (due to the intrinsic uncertainty of the instrument and the problems with the aspect determination) and optical positions. Since we have 132 X-ray sources in our fields we expect to have 1.5 spurious identifications between an X-ray source and a cluster member in our survey, adopting an error circle of $20''$. After proper posi-

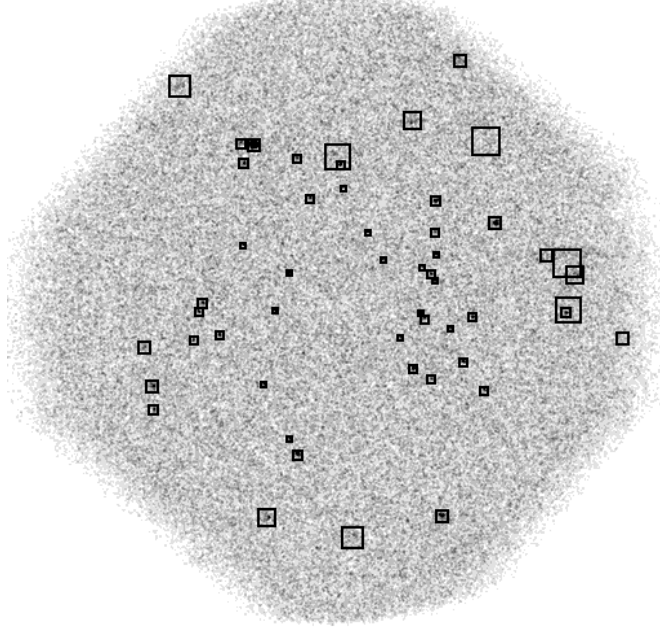


Fig. 2. The same as in Fig. 1 for the Field 2.

tional registration of the three segments we have summed them and have searched for sources in the deeper image so obtained for Field 1. At the end of this process we have dropped from the source list the sources that were due to the presence of a hot spot in segment 2 of the field 1. Sources in Field 1 and 2 have been cross-matched with the list of known cluster members and with a list of other objects in the surveyed region adopting a positional matching radius of $20''$. As a result of this analysis we have found 132 X-ray sources, 42 of which are identified with known cluster members, 30 in the Field 1 and 12 in Field 2. Two sources are identified with field stars, while the remaining 88 are unidentified with catalogued objects.

The final sources are indicated with square symbols in Figs. 1 and 2. The size of the squares is proportional to the spatial scale at which the source has been detected with the highest significance. As expected on average the size of the squares increases with offaxis angle as do the PSF, but there are an handful of sources with sizes significantly larger than the local width of the PSF, that are likely extended.

We have computed the expected number of field sources in our fields, using the sensitivity maps obtained by the wavelet algorithm with a spatial resolution of $10'' \times 10''$. We have estimated the number of expected sources un-related to the cluster for a hydrogen column $N_H = 2 \cdot 10^{20} \text{ cm}^{-2}$, obtained interpolating data from Stark et al. (1992) at the Blanco 1 position, and a power-law spectrum with a photon index ranging between 1 and 2. The total number of expected sources in our survey ranges between 13.6 and 19.1, depending on the assumed spectrum, if we use the $\log(N) - \log(S)$ of Branduardi-Raymont et al. (1994), and between 15.4 and 21.5 with the $\log(N) - \log(S)$ of Hasinger et al. (1993). Hence we expect that only a small fraction (of the order of 20%) of the unidentified sources are background extragalactic sources and field stars, while all the

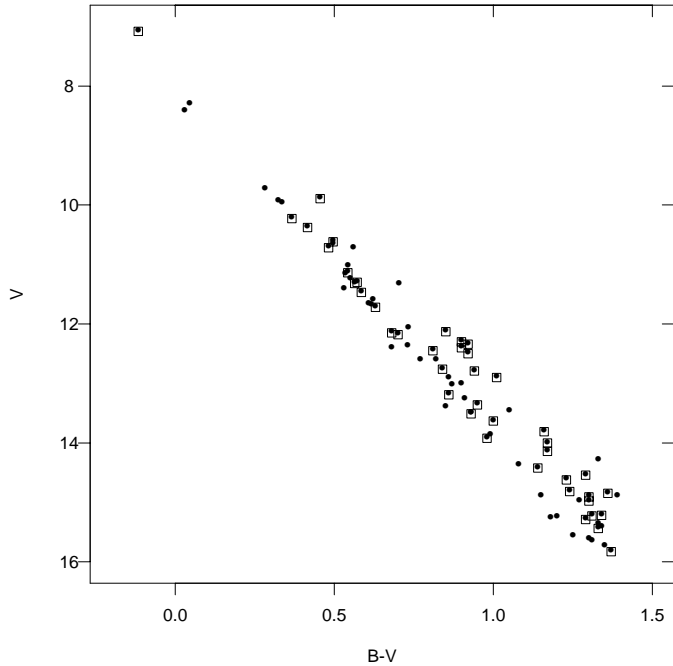


Fig. 3. Color-magnitude diagram of Blanco 1 members falling in the X-ray observed region. Large symbols indicate stars identified with X-ray sources

others will be, likely, new cluster members. Further discussion about the unidentified sources is presented in Sect. 5.

To convert count rates to fluxes we have adopted a conversion factor from HRI count rates to flux (in the 0.1–2.4 keV bandpass) of 3.2×10^{-11} erg cm $^{-2}$ cnt $^{-1}$. It has been derived assuming a single temperature Raymond-Smith model for an optically-thin plasma with a temperature of 1 keV, appropriate for describing the emission from young active coronal emitters, and a hydrogen column density $\log(N_H) = 20$, as deduced from the mean measured $E(B - V)$. The systematic error introduced by the uncertainty in temperature can be estimated to be 20%. In deducing X-ray luminosities for cluster members we have adopted the distance of 250 pc, obtained by Panagi & O'Dell (1997). We report in Table 2, X-ray luminosities for the surveyed cluster members. Positions are from Panagi & O'Dell (1997), photometric values, as well as the star numbers are from de Epstein & Epstein (1985). In Table 2 are reported also the offset between the X-ray and optical position, the detection significance in equivalent σ (i.e., same probability as the normal distribution with this value), the X-ray luminosity and the HRI field in which the star has been observed. For the stars observed in field 1 we report the luminosity obtained summing up all the individual segments of observations. A discussion of the values observed in each single part of the observation will be presented in Sect. 4.

3. X-Ray activity among the Blanco 1 members

In Fig. 3 we show the CM diagram for Blanco 1 members falling in the surveyed region. The large symbols indicate the stars that have been identified with an X-ray source. The cluster mem-

bers that we have looked at but not detected in X-rays are 41. Notice that coronal X-ray emission is common over the entire range of spectral types, starting from mid-F, i.e. at the same stellar mass as in other open clusters. We note that in the G and K color range we detect preferentially stars above the main sequence, likely photometric binaries, with essentially all the stars above the sequence identified with X-ray detections, and only half of the stars on the main sequence detected among the G stars. Notwithstanding the different rates of detections the number statistics of our sample and the distribution of upper limits does not allow us to assess with high confidence level the difference between X-ray luminosity distributions of single and binary stars. Deeper observations would be needed to assess (or disprove) such a conclusion.

No such enhancement in X-ray activity of binary stars is observed in the Pleiades (Micela et al. 1996), while a significant difference is observed between the wide binary systems and single stars in the Hyades (Pye et al. 1994).

The only high-mass star detected is HD 225187, the B8 star referred to above. The detection of this star could be due to the presence of the UV leak on the HRI, but comparing the luminosity value, $\log(L_X) = 29.86$, obtained for this star with the HRI observation of the B stars in the Pleiades for which both PSPC and HRI observations are available (Micela et al. 1998, Fig. 4) we deduce that the observed emission for HD 225187 is too high for its spectral type to be explained exclusively on the basis of UV leak. Indeed on the basis of Pleiades observations the UV leak of a B8 star would produce an emission that, if interpreted in terms of X-ray emission, is of the order of $\log(L_X) = 29.3$, 3–4 times less than our measurement. We conclude that some fraction of the emission can be “real” X-ray emission, that could be due to an unseen late-type companion (see for example the discussion about emission in late-B stars in the Pleiades in Micela et al. 1996). We note, however, that HD 225187 is the source we have detected with the smallest significance (4.51σ with a threshold of 4.50σ) and the results relative to this source need to be treated with caution.

The scatter plot of L_X vs. $B - V$ for the detected stars is shown in Fig. 4. The solid horizontal lines indicate the median $\log(L_X)$ for the Pleiades (Stauffer et al. 1994, Micela et al. 1996) for the 0.3–0.5, 0.5–0.8, 0.8–1.45, > 1.45 $B - V$ ranges corresponding to the early dF, dF7–G9, dK0–9, dM0–5 spectral types, respectively. The extremes of the solid vertical lines indicate the 10% and 90% range of the Pleiades $\log(L_X)$ Maximum Likelihood distribution function. For comparison we show with dashed lines the same information for the α Per open cluster (Randich et al. 1996).

The luminosity level and the large spread of L_X for G and K stars is similar to that observed in the Pleiades, indicating similar X-ray properties. In particular in Fig. 5 and 6 we report the maximum likelihood X-ray luminosity functions for G (defined as the stars with $B - V$ color in the 0.5–0.8 range) and K stars ($0.8 < B - V < 1.4$). In these figures are reported also the corresponding distribution function for the Pleiades, obtained by merging all the available X-ray observations (Micela et al. in prep.), and for the α Per cluster (Randich et al. 1996). The

Table 2. X-ray properties of cluster members.

No.	R.A(J2000) (h. m. s.)	DEC(J2000) °, ′, ″	V	B – V	Offset ″	σ	log(L_X) (erg/sec)	Field
30	0:01:39.3	–29:52:27.2	12.41	0.68	<29.52	1
35	0:01:39.8	–30:04:39.1	14.42	1.14	14.34	7.05	29.85	1
36	0:01:46.4	–29:51:48.8	15.62	1.30	<29.44	1
37	0:01:53.4	–30:06:13.6	15.29	1.29	2.82	7.42	29.29	1
38	0:01:54.4	–30:07:42.4	13.63	1.00	1.09	17.72	29.86	1
39	0:01:57.8	–30:09:30.8	9.97	0.335	<29.37	1
40	0:01:56.9	–30:12:08.8	14.98	1.30	10.04	5.00	29.45	1
42	0:02:04.3	–30:10:35.2	14.14	1.17	4.45	7.38	29.57	1
43	0:02:03.9	–30:10:24.6	14.91	1.30	8.84	7.38	29.57	1
44	0:02:14.5	–29:48:58.6	13.19	0.86	0.01	9.92	29.59	1
45	0:02:19.1	–29:51:08.1	12.76	0.84	11.63	4.94	29.20	1
46	0:02:19.7	–29:56:08.3	14.00	1.17	3.90	13.37	29.46	1
48	0:02:21.6	–30:08:22.6	10.72	0.482	1.73	22.59	29.85	1
49	0:02:11.9	–30:15:03.5	9.89	0.455	5.65	16.90	30.16	1
52	0:02:30.9	–30:17:02.9	15.65	1.31	<29.62	1
53	0:02:24.3	–30:09:10.1	15.57	1.25	<29.09	1
54	0:02:28.2	–30:04:44.4	12.90	1.01	2.26	23.14	29.76	1
55	0:02:21.4	–29:47:49.8	10.73	0.56	<29.29	1
56	0:02:27.3	–29:46:54.0	11.17	0.535	<29.31	1
57	0:02:20.7	–29:45:54.1	11.69	0.616	<29.41	1
58	0:01:46.5	–29:46:39.9	12.15	0.68	12.95	5.49	29.82	1
60	0:02:41.8	–29:58:53.7	15.22	1.34	2.49	6.00	29.14	1
61	0:02:34.8	–30:05:26.4	13.51	0.93	2.42	33.62	30.00	1
62	0:02:36.4	–30:07:05.9	12.45	0.81	15.77	11.99	29.46	1
68	0:02:44.6	–30:13:09.2	14.91	1.15	<29.26	1
70	0:02:48.2	–29:46:35.8	13.51	0.93	<29.30	1
71	0:03:02.9	–29:47:44.9	14.54	1.29	6.09	9.83	29.56	1
72	0:02:57.5	–29:48:30.3	13.40	0.85	<29.17	1
73	0:02:59.4	–29:52:54.8	15.42	1.34	<28.87	1
74	0:03:04.2	–30:00:09.3	15.28	1.18	<28.76	1
75	0:03:00.3	–30:03:22.3	12.79	0.94	1.52	18.90	29.62	1
76	0:02:56.4	–30:04:45.6	12.13	0.85	0.90	52.33	30.26	1
77	0:02:55.1	–30:08:53.8	8.43	0.03	<28.96	1
83	0:03:07.1	–30:15:17.9	12.50	0.92	8.56	6.84	29.40	1
84	0:03:10.9	–30:10:51.0	11.32	0.564	3.25	11.41	29.58	1
88	0:03:06.6	–29:43:12.5	13.81	1.16	4.15	8.17	29.80	1
89	0:03:18.7	–29:44:43.3	14.37	1.08	<29.51	1
90	0:03:24.4	–29:48:49.0	10.62	0.496	0.61	10.17	29.61	1
91	0:03:20.6	–29:49:22.8	11.30	0.572	0.79	9.30	29.51	1
92	0:03:24.9	–29:53:13.9	14.98	1.27	<29.10	1
93	0:03:24.7	–29:55:15.5	13.92	0.98	1.98	9.45	29.32	1
94	0:03:24.2	–29:56:23.7	14.62	1.23	1.07	4.73	28.77	1
95	0:03:16.5	–29:58:48.1	12.34	0.92	1.73	6.87	28.96	1
96	0:03:22.0	–30:01:09.7	10.38	0.416	1.42	14.75	29.54	1
104	0:03:31.9	–29:43:04.8	10.23	0.366	17.63	4.79	29.79	1
105	0:03:39.8	–30:02:10.2	11.42	0.53	<29.14	1
107	0:03:50.2	–30:03:56.3	11.04	0.543	<29.34	1
111	0:04:07.6	–30:06:35.8	12.62	0.82	<29.72	2
112	0:04:04.0	–29:58:27.5	13.02	0.90	<29.82	1
113	0:04:07.7	–29:53:01.2	12.92	0.86	<29.89	1
W71	0:04:11.7	–30:08:05.7	7.08	–0.117	11.58	4.51	29.86	2
115	0:04:12.5	–29:58:02.4	15.83	1.37	10.34	10.73	30.03	1
128	0:04:38.6	–30:00:57.8	15.74	1.35	<29.32	2
129	0:04:31.8	–30:14:42.5	11.68	0.608	<29.59	2
133	0:04:49.0	–30:01:19.7	14.30	1.33	<29.17	2
134	0:04:49.2	–30:00:56.3	11.14	0.542	7.49	17.7	29.82	2

Table 2. (continued)

No.	R.A(J2000) (h. m. s.)	DEC(J2000) ° ' "	<i>V</i>	<i>B</i> – <i>V</i>	Offset "	σ	$\log(L_X)$ (erg/sec)	Field
138	0:04:58.8	–30:09:42.4	11.47	0.585	1.62	10.33	29.38	2
139	0:04:53.0	–30:15:19.5	8.31	0.045	<29.32	2
142	0:05:04.8	–30:19:40.0	15.23	1.31	2.41	12.46	29.73	2
144	0:05:07.1	–29:59:26.7	14.82	1.24	2.86	12.4	29.59	2
147	0:05:17.6	–29:46:58.3	13.26	0.91	<29.84	2
148	0:05:14.4	–29:54:26.1	12.30	0.90	13.46	6.28	29.52	2
149	0:05:13.0	–29:55:31.4	14.91	1.39	<29.21	2
151	0:05:20.2	–30:25:22.7	13.03	0.87	<29.95	2
153	0:05:23.5	–30:23:33.4	12.38	0.73	<29.71	2
154	0:05:31.6	–30:20:52.6	13.36	0.95	8.64	4.98	29.60	2
155	0:05:23.8	–30:19:55.6	15.25	1.20	<29.42	2
156	0:05:25.5	–30:18:36.5	15.37	1.33	<29.33	2
157	0:05:26.7	–30:17:24.9	9.73	0.282	<29.22	2
158	0:05:29.0	–30:08:33.0	13.47	1.05	<28.79	2
159	0:05:29.2	–30:06:54.2	11.33	0.703	<28.80	2
160	0:05:30.9	–29:53:09.0	11.26	0.551	<29.30	2
161	0:05:27.0	–29:51:21.6	12.61	0.77	<29.43	2
165	0:05:35.5	–29:57:07.5	12.40	0.90	3.29	11.90	29.45	2
166	0:05:42.9	–29:57:39.0	9.94	0.324	<28.99	2
167	0:05:35.1	–30:02:11.1	12.07	0.733	<28.82	2
170	0:05:54.7	–30:06:26.8	12.18	0.70	2.58	8.82	29.21	2
171	0:05:54.8	–30:04:39.7	10.67	0.496	<28.81	2
172	0:06:04.3	–30:02:12.8	15.44	1.33	3.50	7.95	29.11	2
182	0:06:16.3	–30:05:58.0	11.72	0.629	5.21	7.34	29.31	2
184	0:06:23.9	–29:52:04.2	14.85	1.36	7.19	7.10	29.79	2
187	0:06:30.2	–29:53:18.7	13.87	0.99	<29.68	2
189	0:06:28.6	–30:17:49.9	11.61	0.622	<29.59	2

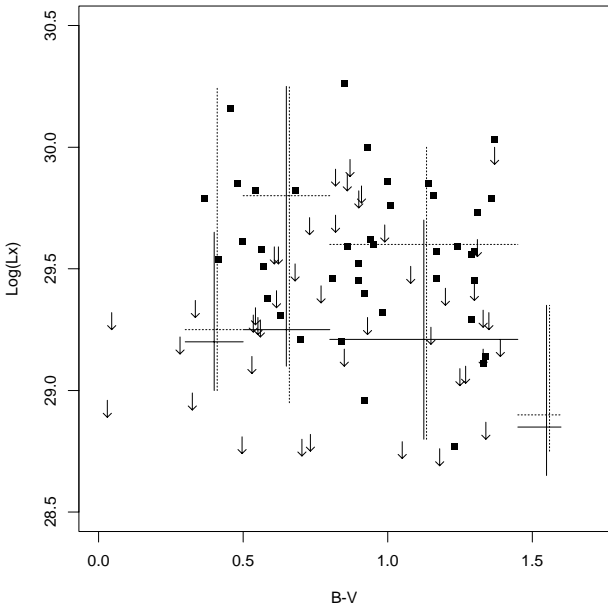


Fig. 4. Scatter plot of L_X vs. B – V for Blanco 1 likely members detected in X-ray. The solid horizontal lines indicate the median $\log(L_X)$ for the Pleiades, while the dashed lines indicate the median for the α Per cluster. Vertical lines indicate the 10% and 90% inter-quantile ranges for the two clusters.

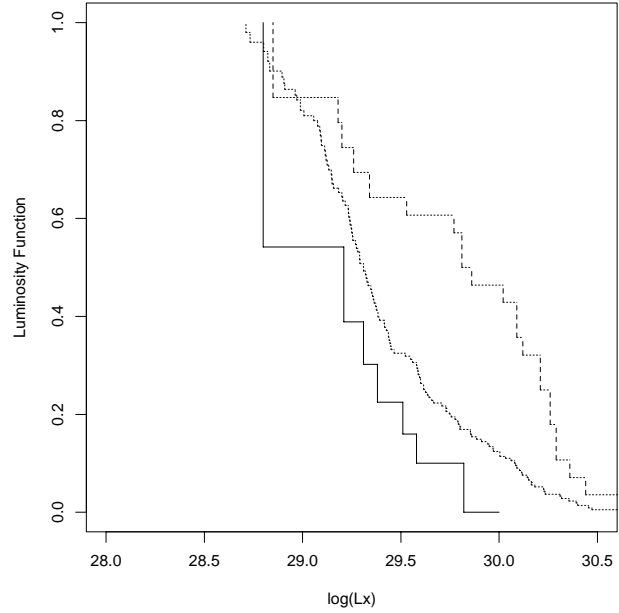


Fig. 5. Maximum likelihood distribution of X-ray luminosity function of G stars of Blanco 1 (continuous line). Dotted and dashed lines are the analogous distributions for G stars in the Pleiades and α Per, respectively. Note that the distribution of the Blanco 1 stars is consistent with that of the Pleiades and much lower than that of α Per.

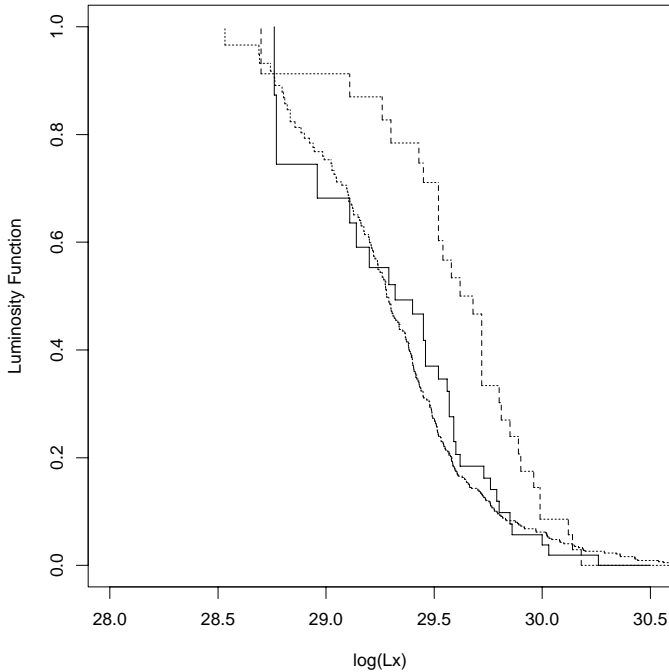


Fig. 6. Maximum likelihood distribution of X-ray luminosity function of K stars of Blanco 1 (continuous line). Dotted and dashed lines are the analogous distributions for K stars in the Pleiades and α Per, respectively. Also in this case the distribution of the Blanco 1 stars is consistent with that of the Pleiades and much lower than that of α Per.

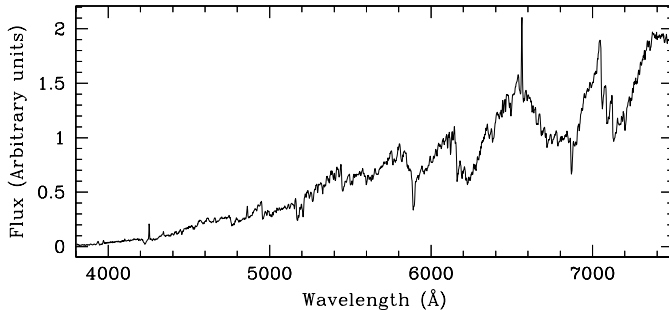


Fig. 7. Optical spectrum of the counterpart of source BLX-26 obtained at ESO 1.5m telescope

Blanco 1 stars are much less luminous than stars in α Per. A two sample test allows to reject the hypothesis that stars of the two clusters are drawn from the same parent population at high confidence level ($> 99.7\%$ and $> 99.6\%$ for K and G stars, respectively), strongly suggesting than Blanco 1 is older than α Per. Comparing the luminosity functions of Blanco 1 with those of the Pleiades a two sample test allows us to reject the hypothesis that the L_x distributions of the G stars in the Pleiades are not drawn from the same parent population only with a confidence level ranging from 93% to 97% depending on the adopted test. This confidence level is not very high but suggests that the G stars of Blanco 1 tend to be slightly less luminous than the analogous stars in the Pleiades, while the K stars are indistinguishable. This possible different behavior between G and K stars would be consistent with the hypothesis

Table 3. L_x of cluster members measured in the three temporal segments of Field 1 with at least one detection. Asterisks indicate the observational segments showing significant short-term variability.

No	V	B - V	Log($L_{x,1}$) (erg/sec)	Log($L_{x,2}$) (erg/sec)	Log($L_{x,3}$) (erg/sec)	Note
37	15.29	1.29	29.46	<29.68	29.39	NV
38	13.63	1.00	30.05	29.92*	30.11	$V > 99.9$
42	14.14	1.17	<29.59	29.73	29.75	NV
43	14.91	1.30	<29.59	29.73	29.75	NV
44	13.19	0.86	29.59	29.58	29.69	NV
46	14	1.17	29.44	29.37	29.45	NV
48	10.72	0.482	29.81	29.82	29.76	NV
49	9.89	0.455	30.22	30.14	30.12*	NV
54	12.9	1.01	29.79	29.87	29.7	NV
60	15.22	1.34	<29.01	<29.18	29.12	NV
61	13.51	0.93	30.01*	29.75	30.04	$V > 99.9$
62	12.45	0.81	29.56*	29.59	29.4	NV
71	14.54	1.29	29.56	29.49	29.65	NV
75	12.79	0.94	29.31	29.71	29.69*	$V > 99.5$
76	12.13	0.85	30.24*	30.36*	30.24	$V > 92.8$
83	12.5	0.92	29.63	<29.83	<29.66	NV
84	11.32	0.564	29.77	<29.58	29.6	NV
88	13.81	1.16	29.97	<30	<29.74	NV
90	10.62	0.496	29.59	29.7	29.48	NV
91	11.3	0.572	29.42	<29.69	29.59	NV
93	13.92	0.98	29.29	29.32	29.28	NV
95	12.34	0.92	<29.11	<29.2	29.07	NV
96	10.38	0.416	29.66	29.54	29.41	NV
112	13.02	0.9	29.75	<30.08	<29.71	NV
115	15.83	1.37	<30.01	30.56*	<29.91	($V > 99.8$)

The variability test for star 115 is unreliable since the rate measured in segment 2 is affected by the hot spot of HRI

that the time scale of the decline of activity with age depends on stellar mass (see for example Randich 1997), in the sense that the higher mass stars decrease their luminosity more rapidly than the lower mass stars. This is consistent with the age of Blanco 1 being slightly greater than the Pleiades in agreement with the results based on the number of H α emitters of Panagi & O'Dell (1997).

We miss totally the dM stars, due to the limiting magnitude of the optical reference catalog, and we expect that a large fraction of the X-ray emitters detected in our observation and not yet identified are actually low-mass cluster members. We have started an optical observational campaign to identify these potential new members and the first observations indicate that many of the optical counterparts are indeed dMe stars with visual magnitude consistent with the cluster distance (see Sect. 5).

4. X-ray variability of cluster members

Field 1 has been observed in three different time segments ≈ 6 months apart. This circumstance allows us to explore X-ray variability on this time scale. Indeed for some sources, variability of the activity level is observed from one segment to the other as reported in Table 3, where we list the various values of

Table 4. X-ray properties of non identified X-ray sources.

Name	R.A.(J2000) (h.m.s.)	DEC.(J2000) ($^{\circ}$ $'$ $''$)	σ	Rate cts/ksec	Err	Notes
BLX-01	0:01:27.1	-29:55:10.6	15.30	7.87	1.63	
BLX-02	0:01:43.7	-29:54:41.2	5.09	1.40	0.41	
BLX-03	0:01:47.4	-30:04:21.3	5.19	1.45	0.41	
BLX-04	0:01:56.2	-30:07:31.5	6.72	0.73	0.21	
BLX-05	0:01:59.4	-29:50:11.9	4.98	5.80	1.63	Only segm. 3
BLX-06	0:01:59.4	-29:58:41.6	5.90	2.87	0.75	Extended
BLX-07	0:02:00.2	-29:59:16.6	9.01	1.10	0.19	
BLX-08	0:02:00.2	-29:51:16.6	7.47	1.08	0.28	
BLX-09	0:02:00.6	-29:57:56.7	7.38	0.98	0.25	
BLX-10	0:02:01.4	-29:52:36.7	6.34	0.87	0.24	
BLX-11	0:02:05.0	-30:10:17.1	4.77	2.23	0.73	Only segm. 2
BLX-12	0:02:07.2	-30:04:41.8	4.87	0.35	0.12	
BLX-13	0:02:11.5	-30:07:01.9	7.53	0.80	0.21	
BLX-14	0:02:11.9	-30:02:34.4	5.48	0.52	0.16	
BLX-15	0:02:22.3	-30:02:52.0	8.29	0.49	0.13	
BLX-16	0:02:23.1	-29:50:34.5	6.31	0.48	0.14	
BLX-17	0:02:25.2	-29:52:34.6	6.79	0.50	0.13	
BLX-18	0:02:31.7	-30:06:37.1	6.20	0.35	0.11	
BLX-19	0:02:34.8	-29:55:54.6	5.82	0.31	0.10	
BLX-20	0:02:35.9	-29:52:42.5	4.69	1.15	0.40	Only segm. 2
BLX-21	0:02:38.5	-29:57:39.7	8.92	0.59	0.11	
BLX-22	0:02:38.8	-30:08:04.7	4.72	0.34	0.11	
BLX-23	0:02:45.0	-29:54:59.7	7.57	0.57	0.15	
BLX-24	0:02:47.9	-29:53:49.7	6.52	0.48	0.14	
BLX-25	0:02:48.2	-29:55:17.5	5.34	5.96	1.59	Only segm. 3
BLX-26	0:02:51.0	-29:54:47.2	5.93	0.59	0.17	
BLX-27	0:02:53.7	-30:06:57.2	8.52	0.67	0.17	
BLX-28	0:02:54.7	-30:09:27.5	4.60	1.02	0.33	Only segm. 3
BLX-29	0:02:55.1	-29:55:12.5	4.94	5.52	1.55	Only segm. 1
BLX-30	0:02:58.3	-30:11:17.2	4.61	0.88	0.27	
BLX-31	0:02:59.8	-29:49:37.2	6.35	0.90	0.24	
BLX-32	0:02:59.8	-29:52:37.1	4.55	0.32	0.11	
BLX-33	0:02:59.8	-29:55:37.1	5.15	2.61	0.72	Extended
BLX-34	0:02:59.8	-30:15:37.1	4.99	1.06	0.31	
BLX-35	0:03:01.7	-29:55:47.1	5.77	0.81	0.22	Extended
BLX-36	0:03:02.3	-29:54:19.6	7.08	0.54	0.15	
BLX-37	0:03:11.3	-29:58:07.4	6.44	0.60	0.20	Only segm. 3
BLX-38	0:03:14.1	-30:06:07.0	6.58	0.48	0.14	
BLX-39	0:03:17.9	-29:58:42.0	6.36	0.35	0.11	
BLX-40	0:03:18.9	-30:02:17.0	6.85	0.49	0.14	
BLX-41	0:03:20.2	-30:04:51.9	4.97	0.65	0.20	
BLX-42	0:03:22.3	-29:53:49.4	10.68	1.18	0.18	
BLX-43	0:03:24.9	-30:12:26.9	7.60	1.16	0.29	
BLX-44	0:03:29.3	-29:53:42.1	4.76	1.73	0.59	Only segm. 2
BLX-45	0:03:29.7	-30:01:19.3	15.70	1.59	0.18	
BLX-46	0:03:34.4	-29:58:31.7	5.55	1.02	0.29	
BLX-47	0:03:34.5	-30:08:06.7	4.88	1.29	0.38	

Table 4. (continued)

Name	R.A.(J2000) (h.m.s.)	DEC.(J2000) ($^{\circ}$ $'$ $''$)	σ	Rate cts/ksec	Err	Notes
BLX-48	0:03:49.5	-30:08:21.6	5.52	10.85	2.93	Only segm. 2
BLX-49	0:03:57.2	-30:03:26.0	63.80	21.54	0.64	
BLX-50	0:04:24.9	-30:04:06.3	4.80	1.19	0.37	
BLX-51	0:04:26.8	-30:06:21.4	4.67	2.94	0.87	
BLX-52	0:04:27.3	-30:03:21.4	9.01	8.22	1.83	Extended
BLX-53	0:04:27.6	-30:06:31.4	6.53	0.84	0.23	
BLX-54	0:04:33.4	-30:02:51.6	4.73	2.10	0.61	
BLX-55	0:04:51.6	-29:55:32.0	4.67	3.84	1.12	Extended
BLX-56	0:04:52.0	-30:11:32.0	6.24	0.54	0.16	
BLX-57	0:04:55.5	-30:06:49.6	7.92	0.66	0.18	
BLX-58	0:04:59.3	-29:50:22.2	8.75	4.32	1.00	
BLX-59	0:05:02.3	-30:07:34.7	5.15	0.30	0.10	
BLX-60	0:05:06.3	-30:02:47.3	8.02	0.52	0.14	
BLX-61	0:05:06.9	-30:01:22.3	4.77	0.37	0.12	
BLX-62	0:05:06.9	-30:04:27.3	9.97	0.83	0.14	
BLX-63	0:05:07.9	-30:10:49.8	5.38	0.43	0.14	
BLX-64	0:05:08.1	-30:04:04.8	6.74	0.55	0.16	
BLX-65	0:05:10.0	-30:06:57.3	4.92	0.38	0.13	
BLX-66	0:05:10.6	-30:03:37.3	4.89	0.29	0.10	
BLX-67	0:05:11.1	-30:06:32.4	52.10	9.67	0.38	
BLX-68	0:05:13.3	-30:10:09.9	10.63	0.88	0.15	
BLX-69	0:05:17.3	-30:08:09.9	5.52	0.33	0.11	
BLX-70	0:05:22.3	-30:03:07.5	4.91	0.29	0.11	
BLX-71	0:05:26.8	-30:01:22.5	19.14	1.88	0.18	
BLX-72	0:05:34.3	-29:58:32.5	5.25	0.32	0.12	
BLX-73	0:05:35.8	-29:56:32.5	4.83	2.89	0.83	Extended
BLX-74	0:05:44.1	-29:59:12.5	6.74	0.58	0.17	
BLX-75	0:05:47.8	-30:15:40.0	14.12	1.69	0.21	
BLX-76	0:05:48.1	-29:56:37.5	5.62	0.48	0.15	
BLX-77	0:05:50.3	-30:14:37.5	7.99	0.55	0.15	
BLX-78	0:05:50.4	-30:03:59.9	9.49	0.75	0.13	
BLX-79	0:05:58.0	-30:11:07.4	6.18	0.40	0.12	
BLX-80	0:06:00.8	-29:55:47.4	59.98	15.15	0.52	
BLX-81	0:06:03.9	-29:56:57.3	8.54	0.99	0.19	
BLX-82	0:06:04.8	-29:55:39.8	5.80	0.67	0.20	
BLX-83	0:06:11.3	-30:07:59.7	8.44	0.66	0.13	
BLX-84	0:06:17.4	-30:06:29.6	7.25	0.63	0.18	
BLX-85	0:06:19.0	-30:08:19.6	5.72	0.47	0.15	
BLX-86	0:06:31.0	-30:12:46.8	5.96	0.72	0.21	
BLX-87	0:06:31.3	-30:11:16.8	10.78	1.84	0.27	
BLX-88	0:06:33.6	-30:08:46.7	5.22	0.81	0.25	

L_X measured for known cluster members detected at least once in one of the segments which compose the X-ray observation of field 1. The last column indicates if the star shows a highly significant change in its X-ray luminosity from one observation to the other, according to a χ^2 analysis. Long-term variability in L_X , at levels up to factors $\approx 2-3$ is evident for a few sources. One star (#112) was not detected in the summed exposure, but was detected in segment 1 alone. In this case the detection is consistent with the upper limit obtained in the summed exposure, since this last exposure is affected by the presence of a hot spot near the source position in segment 2. Similar results

have been obtained on stars of IC4665 (Giampapa et al. 1998), showing variation on a time-scale of one year, without evidence of short-term variability.

We have also looked in detail at the light curves of all the sources listed in Table 3 searching for short-term variability. The individual observations showing evidence for variability (at significance level greater than 99%, as obtained from a Kolmogoroff-Smirnov test) are marked with an asterisk. In some cases both long and short-term variability are present in the same star. The long-term variability cannot be accounted for simply by the occurrence of short-term (flare-like) variability, since in most cases there is no evidence of short term variability within the segment of observations responsible for the long term variations. For example, the star 61 shows short term variability in segment 1, while the long term variation appears to be due to the low value of the luminosity in segment 2, while in segment 3 the star has the same X-ray luminosity as in segment 1, but without evidence for short-term variability.

Variability (either short- or long-term) is detected in about 25% of the K stars and in more than 50% of the K stars observed at high statistical significance (σ equivalent in the summed exposure greater than 10). We do not detect variability in F and G stars observed with similar significance, but the size of F and G star sample is too small to derive strong statistical conclusions. Our results suggest that long-term variability is present at least in the dK stars of Blanco 1 at level comparable with that observed in K stars in the Pleiades (Micela et al. in prep.)

5. Unidentified x-ray sources

We have detected 88 X-ray sources not identified with known cluster members. In Table 4 we report the X-ray properties of unidentified sources, with the σ equivalent of the significance of the detection and the source count rates, while in Fig. 8 we report the finding charts for our non-identified sources. Some of the sources show no visible counterparts in their error circle, and it is possible that a few of them are spurious sources. But also among these “empty” sources there are sources detected at very high signal to noise ratio as for example the source BLX-52, detected with a σ equivalent of 9.01. The wavelet algorithm finds that this source is extended, suggesting that the emission could be due to a cluster of galaxies projected on the back of Blanco 1. Knowing the limiting magnitude of the Schmidt plates used for the finding charts (about 20), we can estimate a lower limit on the f_x/f_v ratio of +0.8 at the limit of the typical ratio for clusters of galaxies or BL Lac objects observed in the *Einstein* Extended Medium Sensitivity Survey (Stocke et al. 1991). The high value of the f_x/f_v ratio excludes the possibility that the source is a normal star (either field or cluster member).

We expect that about 20% of the unidentified sources are objects unrelated to the cluster, mainly of an extragalactic nature (especially for the “empty” fields, as suggested above), while the remaining ones are likely to belong to the cluster. If this prediction is confirmed, the present X-ray observation will be very relevant to determining the mass function of the cluster since we will double the number of known members in the

explored area and we will be able to define the low-mass end of the cluster mass function. A similar procedure has been applied to other open clusters or star forming regions such as Taurus (Walter et al. 1988), Chameleon (Lawson et al. 1996), Sco-Cen (Sciortino et al. 1998), IC2391 (Patten & Simon 1996), IC2602 (Randich et al. 1995). Furthermore we note that in the Pleiades only about half of the dM stars emit to a level comparable with the sensitivity of our survey, so if the dM stars of Blanco 1 have X-ray luminosities similar to those of the Pleiades (as we can expect given the comparable age of the two clusters) we should have detected only half of the dM stars in Blanco 1. From an inspection of the finding charts we estimate that we have detected about 35 stars with magnitudes consistent with dM stars at the cluster distance. On the basis of the XCount model (Favata et al. 1992, Sciortino et al. 1995) we predict that at our sensitivity we have detected at most two field dM stars, i.e. the contamination with respect to the large number of cluster dM stars will be negligible. Hence we expect that the cluster could contain up to 70 dM stars in the surveyed region. Some preliminary optical observations show that many of the possible counterparts in the appropriate magnitude range are indeed dMe stars highly likely to be cluster members. Fig. 7 shows the optical spectrum of source BLX-26 obtained at ESO 1.5m telescope.

Some of these non-identified sources show evident variability on a time-scale of the order of six months. For example 9 out of 50 unidentified sources detected in the field 1 are detected only in one temporal segment and not in the complete summed-up observation. The variations are mainly observed on long time-scales comparable with the time between the observations. Short-term variability due to evident flare-like activity is clearly observed only on the source BLX-45. This source is detected in segments 1 and 3 (not in segment 2 that is the shortest one) and shows a flare in segment 1, (see Fig. 9), while in segment 3 has an activity level consistent with the quiescent level observed in segment 1. The finding chart of this source shows that it has three possible counterparts.

6. Summary and conclusions

We have presented the results of two deep X-ray exposures on Blanco I. The X-ray characteristics of the cluster are similar to those of the Pleiades, with the G stars marginally slightly less active than in the Pleiades. The luminosity functions of G and K stars are significantly lower than the corresponding functions of α Per members. If we assume that the X-ray luminosity distribution of cluster stars depends only on age, our results confirm that the age of Blanco 1 is similar to the Pleiades age and greater than the α Per age, a conclusion consistent with the work of Panagi & O’Dell (1997) based on H α properties of the cluster members.

We detect a large number of sources not identified with known cluster members. About 20% of these new sources are expected to be field stars and extragalactic sources, while the majority are likely to be new low-mass cluster members as indicated by the optical follow-up observations we have started.

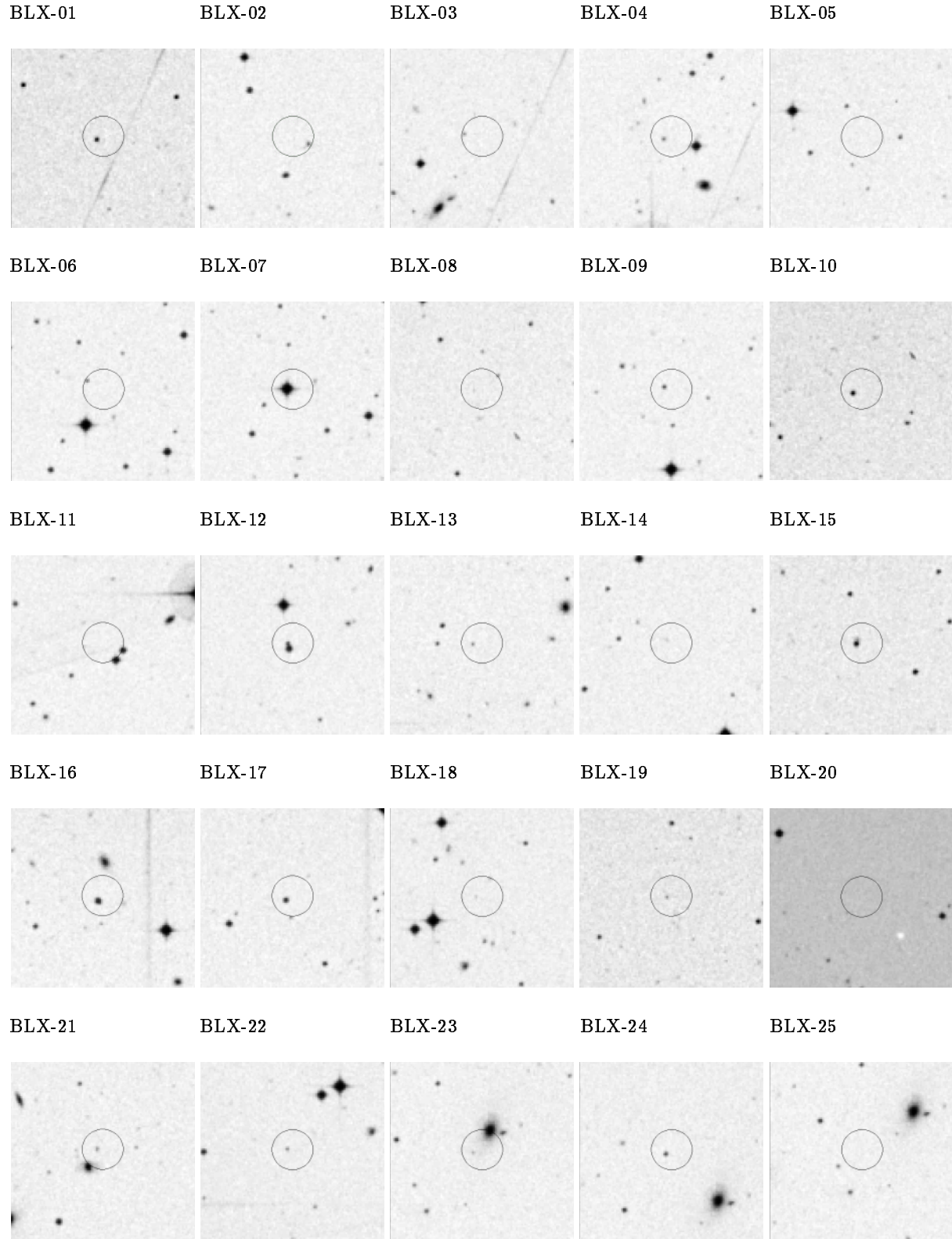


Fig. 8. Finding charts for unidentified HRI sources detected in the Blanco 1 region; star fields extracted from the STScI DSS. Each chart is 3' on a side, centered on the HRI position. Identification circles are indicated.

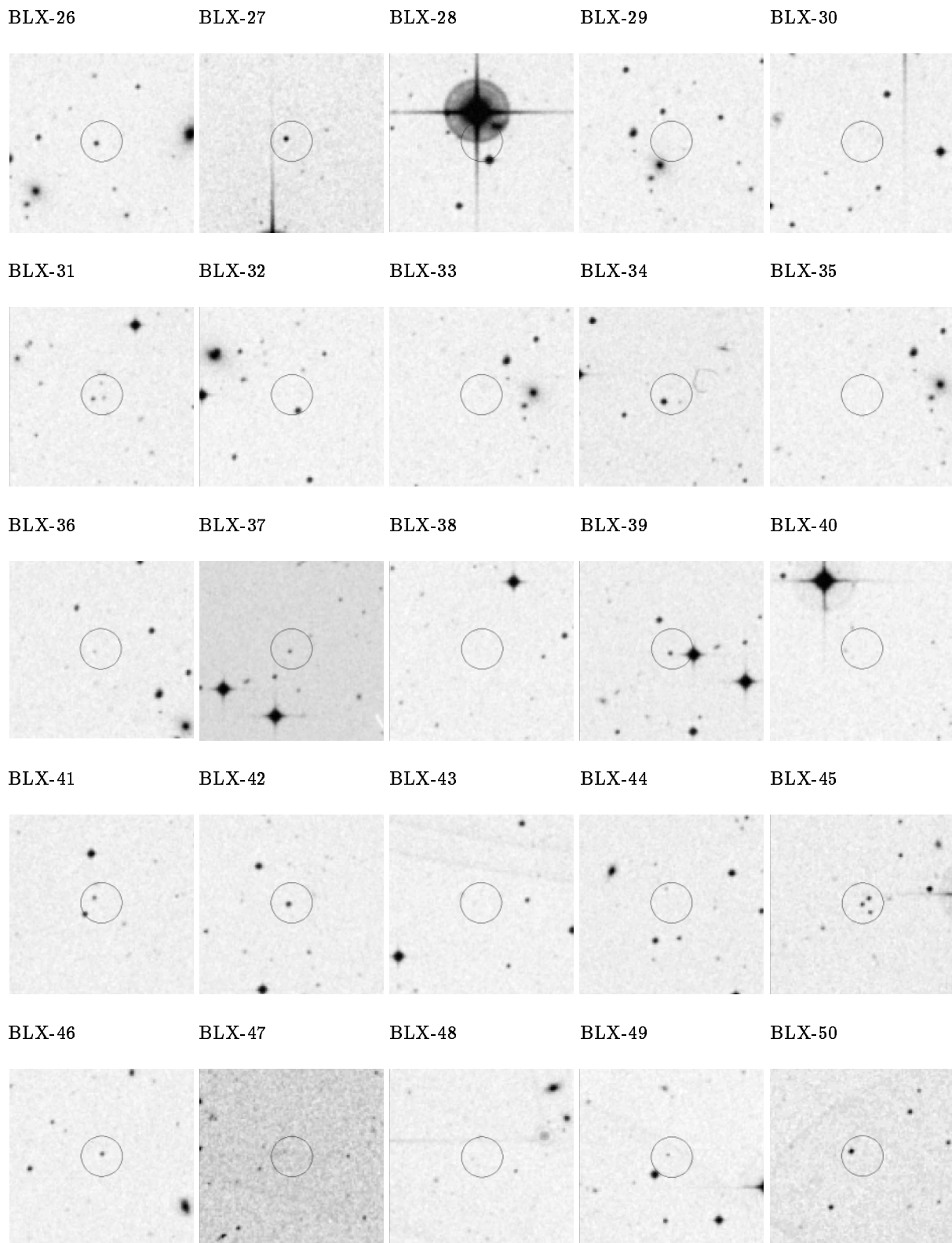


Fig. 8. (continued)

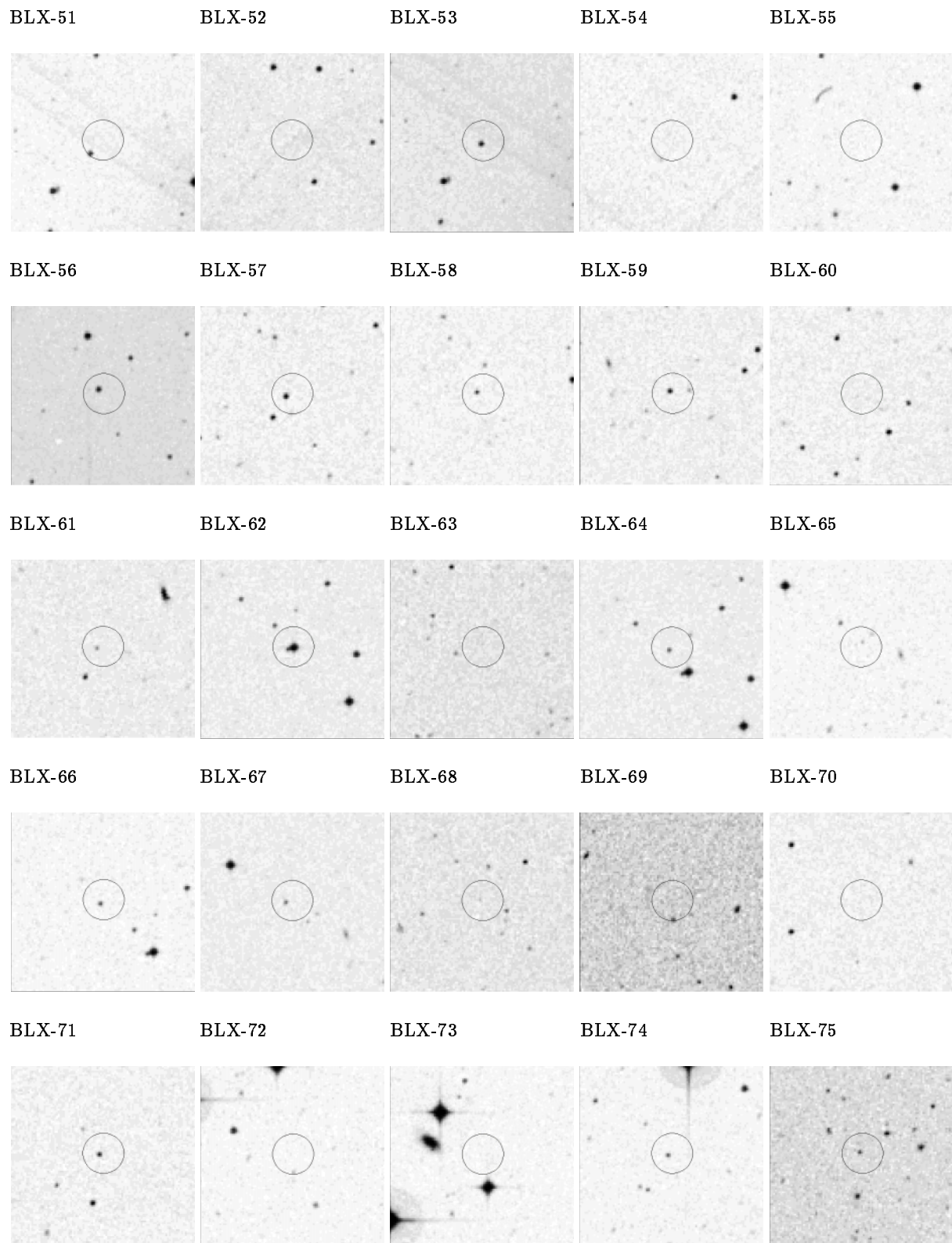


Fig. 8. (continued)

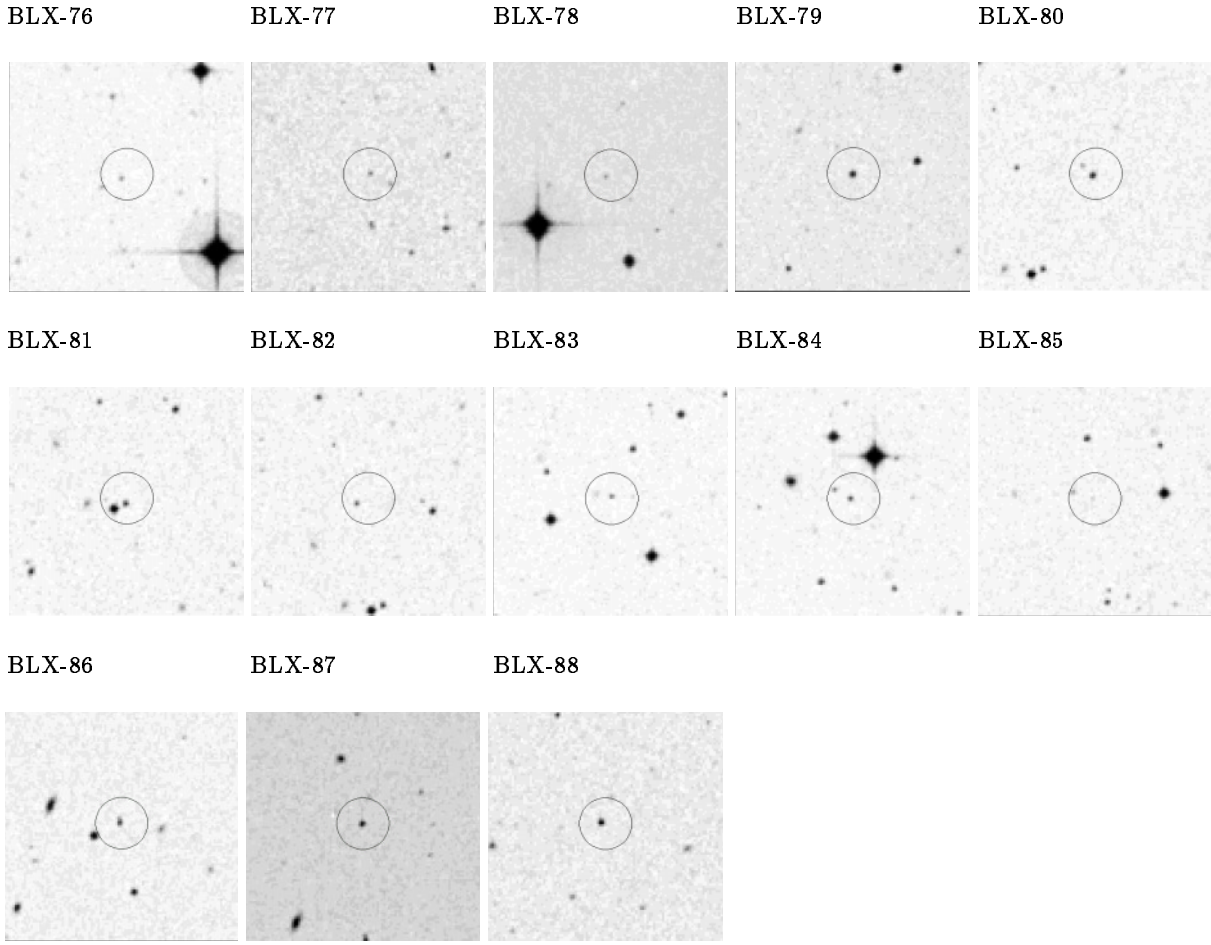


Fig. 8. (continued)

The complete optical identifications of these sources will give a significant improvement in the knowledge of the mass function of Blanco 1.

Long-term variability in L_X , at levels up to factors $\approx 2-3$, is present in 25% of the K stars observed and in more than 50% of the K stars observed with the highest signal to noise ratio and in a fraction of unidentified sources, while a large flare-like event (larger than a factor 30) is detected on one unidentified source suggesting that similar events in the late-type stars of the cluster are exceptional, analogous to the X-ray variability properties of the Pleiades.

Acknowledgements. GM, RP and SS acknowledge financial support from ASI (Italian Space Agency), and MURST (Ministero della Università e della Ricerca Scientifica e Tecnologica). JPP acknowledges the financial support of the UK Particle Physics & Astronomy Research Council. We thank the referee Dr. Corcoran for his useful comments. We acknowledge the usage of the photographic data obtained using The UK Schmidt Telescope and the STScI digitization and compression.

References

Branduardi-Raymont G., Mason K.O., Warwick R.S., et al., 1994, MNRAS 270, 947

Briel U.G., Aschenbach B., Hasinger G., et al., 1996, The ROSAT Users' Handbook

Damiani F., Maggio A., Micela G., Sciortino S., 1997a, ApJ 483, 350

Damiani F., Maggio A., Micela G., Sciortino S., 1997b, ApJ 483, 370

David L.P., Harnden F.R. Jr., Kearns K.E., Zombeck M.V., 1993, The Rosat High Resolution Imager (HRI). U.S. ROSAT Science Data Center/Sao.

de Epstein A.E., Epstein I., 1985, AJ 90, 1211

Edvardsson B., Pettersson B., Kharrazi M., Westerlund B., 1995, A&A 293, 75

Favata F., Micela G., Sciortino S., Vaiana G.S., 1992, A&A 256, 86 1143

Favata F., Micela G., Sciortino S., Morale F., 1997, A&A 324, 998

Giampapa M.S., Warden S.P., Gilliam L.B., 1979, ApJ 229,

Giampapa M.S., Prosser C.F., Fleming T.A., 1998, ApJ in press

Gimenez A., Reglero V., de Castro E., Fernandez-Figueroa M.J., 1991, A&A 248, 563

Gioia I.M., Maccacaro T., Schild R.E., et al., 1990, ApJS 72, 567

Hasinger G., Burg R., Giacconi R., et al., 1993, A&A 275, 1

Jetsu L., Vilhu O., la Dous C., 1990, A&AS 85, 1127

Lawson W.A., Feigelson E.D., Huenemoerder D.P., 1996, MNRAS 280, 1071

Mermilliod J.C., 1997, Mem. Soc. Astron. Ital. 68, 859

Micela G., Sciortino S., Kashyap V., Harnden F.R. Jr., Rosner R., 1996, ApJS 102, 75

Micela G., Sciortino S., Harnden F.R. Jr., et al., 1998, A&A in press

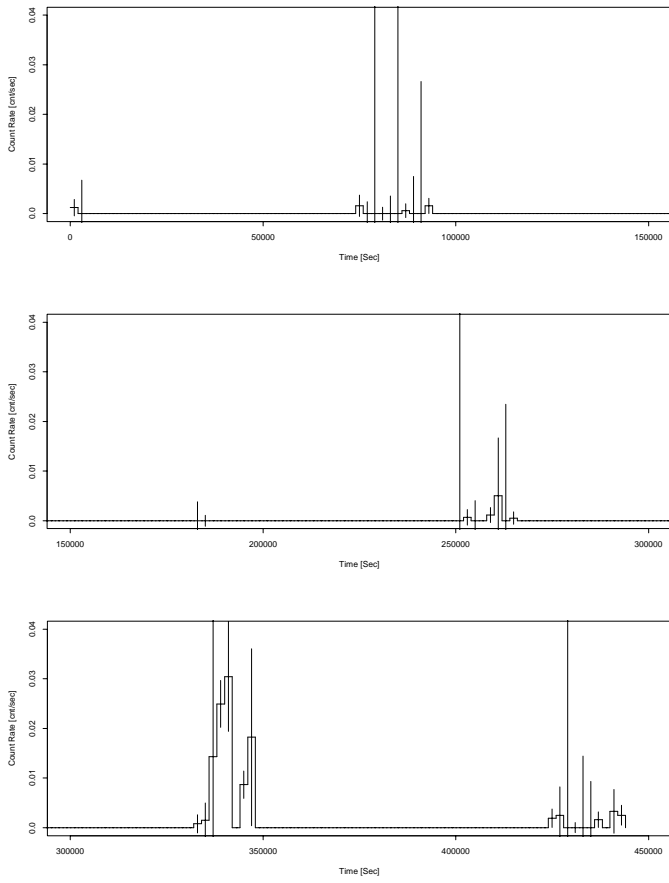


Fig. 9. Light curve of the source BLX-45 observed during the segment 1 showing an evident flare-like event

Morale F., Micela G., Favata F., Sciotino S., 1996, A&AS 119, 403
 Pallavicini R., Golub L., Rosner R., et al., 1981, ApJ 248, 279
 Panagi P.M., O'Dell M.A., 1997, A&AS 121, 213
 Panagi P.M., O'Dell M.A., Collier Cameron A., Robinson R. D., 1994, A&A 292, 439
 Patten B.M., Simon T., 1996, ApJS 106, 489
 Pettersen B.R., 1982, In: Byrne P.D., Rodonò M. (eds.) Proc. of the IAU Coll. 71: Activity in Red Dwarfs Stars. Reidel, Dordrecht, p. 17
 Perry C.L., Walter D.K., Crawford D.L., 1978, PASP 90, 81
 Pye J., Hodgkin S.T., Stern R.A., Stauffer J.R., 1994, MNRAS 266, 798
 Randich S., 1997, Mem. Soc. Astron. Ital. 68, 971
 Randich S., Schmitt J.H.M.M., Prosser C.F., Stauffer J.R., 1995, A&A 300, 134
 Randich S., Schmitt J.H.M.M., Prosser C.F., Stauffer J.R., 1996, A&A 305, 785
 Sciotino S., Favata F., Micela G., 1995, A&A 296, 370
 Sciotino S., Favata F., Damiani F., Micela G., 1998, A&A 332, 825
 Snowden S.L., 1998, ApJS 117, 233
 Snowden S.L., McCammon D., Burrows D.N., Mendenhall J.A., 1994, ApJ 424, 714
 Stark A.A., Gammie, C.F., Wilson, R.W., et al., 1992, ApJS 79, 77
 Stauffer J.R., Caillault J.-P., Gagné M., Prosser C.F., Hartman L.W., 1994, ApJS 91, 625
 Stocke J.T., Morris S.L., Gioia I.M., et al., 1991, ApJS 76, 813
 Walter F.M., Brown A., Mathieu R.D., Myers P.C., Vrba F.J., 1988, AJ 96, 297
 Westerlund B., Garnier R., Lundgren K., Pettersson B., Breysacher J., 1988, A&A 76, 101